This article was downloaded by: *[Kroo, Norbert]*
On: *2 August 2010*
Access details: *Access Details: [subscription number 924800284]*
Publisher *Taylor & Francis*
Informa Ltd Registered in England and Wales Registered Number: 1072954 Registered office: Mortimer House, 37-41 Mortimer Street, London W1T 3JH, UK

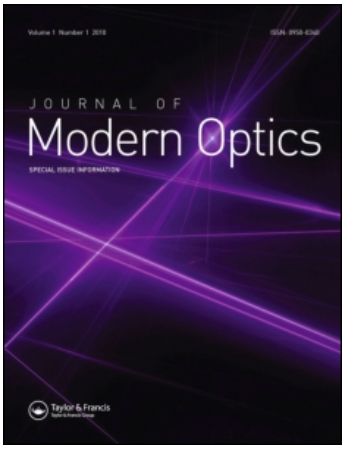

Journal of Modern Optics
Publication details, including instructions for authors and subscription information:
http://www.informaworld.com/smpp/title~content=t713191304

Spontaneous emission of radiation by metallic electrons in the presence of electromagnetic fields of surface plasmon oscillations

Sándor Varró[a]; Norbert Kroó[a]; Gyözö Farkas[a]; Péter Dombi[a]
[a] Research Institute for Solid State Physics and Optics of the Hungarian Academy of Sciences Budapest, Hungary

Online publication date: 03 February 2010

To cite this Article Varró, Sándor , Kroó, Norbert , Farkas, Gyözö and Dombi, Péter(2010) 'Spontaneous emission of radiation by metallic electrons in the presence of electromagnetic fields of surface plasmon oscillations', Journal of Modern Optics, 57: 1, 80 — 90
To link to this Article: DOI: 10.1080/09500340903521835
URL: http://dx.doi.org/10.1080/09500340903521835

PLEASE SCROLL DOWN FOR ARTICLE

Full terms and conditions of use: http://www.informaworld.com/terms-and-conditions-of-access.pdf

This article may be used for research, teaching and private study purposes. Any substantial or systematic reproduction, re-distribution, re-selling, loan or sub-licensing, systematic supply or distribution in any form to anyone is expressly forbidden.

The publisher does not give any warranty express or implied or make any representation that the contents will be complete or accurate or up to date. The accuracy of any instructions, formulae and drug doses should be independently verified with primary sources. The publisher shall not be liable for any loss, actions, claims, proceedings, demand or costs or damages whatsoever or howsoever caused arising directly or indirectly in connection with or arising out of the use of this material.

Journal of Modern Optics
Vol. 57, No. 1, 10 January 2010, 80–90

Taylor & Francis
Taylor & Francis Group

Spontaneous emission of radiation by metallic electrons in the presence of electromagnetic fields of surface plasmon oscillations†

Sándor Varró*, Norbert Kroó, Győző Farkas and Péter Dombi

Research Institute for Solid State Physics and Optics of the Hungarian Academy of Sciences Budapest, Hungary

(*Received 7 May 2009; final version received 30 November 2009*)

The spontaneous emission of metallic electrons embedded in a high-intensity enhanced surface plasmon field is considered analytically. The electrons are described by dressed quantum states which contain the interaction with the plasmon field non-perturbatively. Considerable deviations from the perturbative behaviour have been found in the intensity dependence of the emitted fundamental and the second harmonic signals, even at moderate incoming laser intensities. The theoretical predictions deduced from the formalism are in good qualitative agreement with the experimental results.

Keywords: field enhancement; surface nonlinear optics; surface plasmons

Downloaded By: [Kroo, Norbert] At: 06:04 2 August 2010

1. Introduction

Surface electromagnetic radiation bound to a plane interface separating a dielectric and a conductor started to receive considerable attention just 100 years ago, when a paper by Sommerfeld appeared on the effect of the Earth on the propagation of radio waves [1,2].[1] In the meantime such and similar surface waves have received the name surface plasmon polaritons or surface plasmon oscillations (SPO). As is well known, these oscillatory fields are normal modes of the electromagnetic (EM) radiation in systems consisting of dielectrics (e.g. glass) and conductors (e.g. metals or semiconductors) which are separated by sharp interfaces. Already before the 1960s, the number of theoretical and experimental studies of SPOs was growing fast, and nowadays SPO physics is an important sub-discipline of electrodynamics and optics. On the early development of this branch of research an excellent collection of papers can be found in the books edited by Burstein and de Martini [3] and by Maradudin et al. [4], including many important references. For a good exposition of the subject see also the books by Raether [5]. More recent results are summarised e.g. in the extensive and thoroughly written reports by Zayats and co-workers [6,7]. Surface plasmon physics still raises many fundamental questions concerning radiation–matter interaction and optics [8–16], which are interesting in themselves. At the same time, this rapidly growing field of research will surely impact many branches of science and technology [17].

One of the main characteristics of the SPOs is their very large electromagnetic fields concentrated at the interfaces of metals and dielectrics. To our knowledge, such an enhancement was first discussed by Fano [18] in 1938. Recently this phenomenon has become the subject of extensive research, because on the basis of it high-order nonlinear processes can be induced even at relatively moderate intensities of an incomig radiation which excites the SPOs [19–25]. For instance in [22] the authors report on the observation of high-harmonic generation (HHG) from an argon gas jet, in the extreme ultraviolet, induced by a field of a Ti:Sapphire laser pulse, which was resonantly enhanced through surface plasmons within a metallic nanostructure. As for the theory of such experimental findings, one would think at first glance that, at least from the point of view of the generation itself by a *single atom*, there are no new elements needed to interpret this results, because the interpretation of HHG has long received a well-established theoretical framework [26–28]. However, in the case of surface plasmon excitation the modal structure of the radiation near the surface is considerably different from that in free space, and this circumstance has to be taken into account [29] too. The HHG process induced *directly* by high-intensity laser fields on *metal surfaces* of thick samples has also been a subject of extensive research earlier [30], and both

*Corresponding author. Email: varro@mail.kfki.hu
†This paper is part of the Special Issue, Physics of Quantum Electronics. Selected Papers from the 39th Winter Colloquium on the Physics of Quantum Electronics, 4–8 January 2009, published as Vol. 56, Numbers 18–19, of the *Journal of Modern Optics*.

ISSN 0950–0340 print/ISSN 1362–3044 online
© 2010 Taylor & Francis
DOI: 10.1080/09500340903521835
http://www.informaworld.com

Downloaded By: [Kroo, Norbert] At: 06:04 2 August 2010

classical and quantum mechanical [31,32] interpretations have been worked out. On the other hand, if a *thin metal layer* is excited through a dielectric (say in the Kretschmann geometry [33]), the enhanced field of the generated surface plasmons may govern the light emission process. The light emission can be quite satisfactorily interpreted e.g. as resulting due to the surface roughness, which secures the momentum conservation in the 'light to SPO' and 'SPO to light' conversion processes. In the quantum description there appears an interaction Hamiltonian due to surface roughness which already couples these two different kinds of electromagnetic radiation [34]. Usually the coupling is described by a phenomenological interaction term, and there are several techniques to generate SPOs through surface-geometrical effects, as is summarised e.g. by Zayats et al. [7]. In our present paper we study the quantum mechanical coupling of a strong external plasmon field to the photon field through an assembly of free electrons, and we do not explicitly take into account surface roughness. According to this description, the high-harmonic generation on thin metal films is a result of multiple-plasmon scattering on a free electron gas inside the metal. This may seem to be an analogous process to the multiphoton Compton scattering by free electrons, which has an extensive literature (see e.g. [35] and references therein). More precisely, the process to be considered is spontaneous emission of photons by an electron reflected by the metal surface in the presence of a high-intensity SPO field. At this point let us note that very likely several theoretical approaches, which have long been worked out to treat nonlinear processes taking place directly in high-intensity laser fields, could be implemented in the recent investigations of processes induced by the strong enhanced SPO fields. The present paper may be considered as a contribution belonging to this direction of the theoretical research.

In continuing our recent work on light emission by surface plasmon oscillations [36,37], the immediate motivation for the present study is the apparently strange results of our experiments [38] in which we measured the intensity dependence of light emission (fundamental and second harmonic) generated by a moderately intense laser radiation from a thin film of gold on a glass prism. The measured slope of the signal-intensity curve manifestly deviated from that one would expect on the basis of earlier treatments, even if one takes non-perturbatively into account the field enhancement too. In the following we shall give a theoretical description of the light emission process, in the frame of which the basic features of the above-mentioned experimental results can be interpreted.

In Section 2 we shall briefly summarise the main steps leading to the explicit form of the electromagnetic fields of the SPOs, and give a physical background for the key parameters naturally appearing in the analysis. A particular emphasise shall be put on the clear distinction between the scattering (evanescent) waves of the EM radiation and the SPO fields generated at the metal–vacuum interface. Section 3 is devoted to the discussion of the general analytic form and physical content of the wave functions of an electron dressed by the surface plasmon field. In Section 4 the transition probabilities of the spontaneous emission of photons by an electron reflected at the metal surface in the presence of the high-intensity SPO field are given. The analytic results obtained shall be used in a few numerical examples to illustrate the intensity dependence, the degree of nonlinearity and the angular distribution of the emitted light signal. In Section 5 a brief summary closes our paper.

2. Generation of the enhanced scattering fields and SPOs

In the present section we give a quantitative picture of the enhanced fields appearing at plane interfaces separating a metal layer and dielectrics. The spatial distribution of the SPO fields in single- and multiple-film structures and their dispersion relations have been investigated in detail, for example, by Economou for lossless systems [39]. Burke et al. [40] have given a thorough analysis of propagation of SPO-like waves guided by thin, lossy metal films, and they have also discussed the question of wave launching. Here we will not enter into the discussion of this important problem, rather, we shall merely summarise the basic 'kinematic' characterisation of the fields.

In the Kretschmann geometry [33] we have to consider the solutions of the Maxwell equations in three regions shown in Figure 1. Region 1 ($z>d$) is filled with a dielectric, which represents e.g. a glass prism of index of refraction $n_1 = \varepsilon_1^{1/2}$. The metal layer occupies region 2 ($0<z<d$) of thickness d and of (in general complex) dielectric constant $\varepsilon_2 = n_2^2$. In the experiments region 3 ($z<0$) is often simply air, which can practically be considered as vacuum with the dielectric constant $\varepsilon_3 = 1$. The solutions of the Maxwell equations automatically fall into two classes of independent waves; the transverse magnetic (TM: $\boldsymbol{B}$ is perpendicular to the x–z scattering plane) and the transverse electric (TE: $\boldsymbol{E}$ is perpendicular to the x–z scattering plane) waves, which are also called p-polarised and s-polarised waves, respectively. In each case both E_x and B_y have to be continuous at

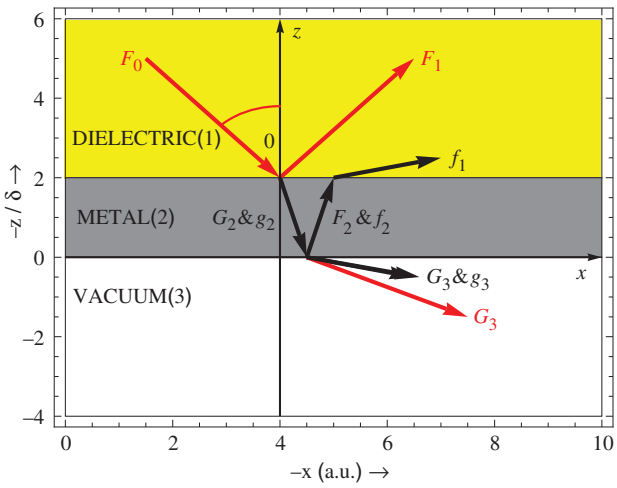

Figure 1. Illustrates the TM electromagnetic field configuration excited by a plane wave of amplitude F_0 impinging on the metal layer from the dielectric an angle of incidence θ_0. The z-coordinate is measured in units of the skin depth δ, which is typically ~22.5 nm in our experiments. The freely propagating waves are symbolised by red arrows, and the evanescent waves are symbolised by black arrows. For further details see the main text. (The colour version of this figure is included in the online version of the journal.)

the glass–metal ($z=d$) and the metal–air ($z=0$) interfaces. If we take a common pure harmonic temporal dependence $\exp(-\mathrm{i}\omega t)$ of the TM fields, then for B_y the Helmholtz equation $(\partial_x^2+\partial_z^2+K^2)B_y=0$ follows, where $K^2\equiv(\omega/c)^2\varepsilon$. In the scattering problem under discussion the fields are usually modelled by superpositions of plane waves of the form $\exp[\mathrm{i}(K_x x+K_z z)]$ with four unknown constant amplitudes determined by the *inhomogeneous* set of linear algebraic equations stemming from the boundary conditions. In Figure 1 the capital letters F_1, G_2, F_2 and G_3 label the reflected, the first refracted, the second reflected and the second refracted (transmitted) waves, respectively. These waves are directly induced by the incoming field of amplitude $F_0\neq 0$, and they represent *scattering states*. If the angle of incidence θ_0 is smaller than the angle of total reflection θ_t (see below), then G_3 represents a free running wave. For θ_0 larger than θ_t, this refracted wave becomes evanescent (bound to the metal–air interface). The small letters f_1, g_2, f_2 and g_3 denote the amplitudes characterizing the SPO *eigenmodes* in the dielectric–metal–vacuum system. They are solutions of a set of *homogeneous* linear algebraic equations ($F_0=0$) whose determinant must vanish in order to have nontrivial solutions. As is suggested in the figure, all these latter waves are evanescent.

According to the above considerations, the complex magnetic induction and the electric field strength of a p-polarised plane wave in regions 1, 2 and 3 can be explicitly expressed as

$$\boldsymbol{B}=\boldsymbol{e_y}B(z)\exp[\mathrm{i}(K_x x-\omega t)],$$
$$\boldsymbol{E}=(c/\mathrm{i}\omega\varepsilon)[\boldsymbol{e_x}\partial_z B(z)-\mathrm{i}\boldsymbol{e_z}K_x B(z)]\exp[\mathrm{i}(K_x x-\omega t)]. \quad (1)$$

Here $\boldsymbol{e_{x,y,z}}$ denote unit vectors pointing along the corresponding positive coordinate axes. In the above equation we can *either* take $K_x=K_0\sin\theta_0$ with $K_0\equiv(\omega_0/c)\varepsilon_1$, *or* $K_x=k_{1x}$, depending on whether we are dealing with scattering waves or with the SPO eigenmodes of wave numbers $k_{\mathrm{sp}}\equiv k_{1x}(\omega)$. The boundary conditions (the continuity of E_x and B_y at the interfaces) are equivalent to the requirement that $B(z)$ and $\partial_z B(z)$ be continuous at both of the planes defined by the relations $z=d$ and $z=0$. As is illustrated in Figure 1, the scattering states are represented by the wave functions

$$B_0(z)\equiv\begin{cases} n_1(F_0\exp(-\mathrm{i}K_{1z}z)+F_1\exp(+\mathrm{i}K_{1z}z)) \\ \quad (z>d), \\ n_2(G_2\exp(-\mathrm{i}K_{2z}z)+F_2\exp(+\mathrm{i}K_{2z}z)) \\ \quad (0<z<d), \\ n_3G_3\exp(-\mathrm{i}K_{3z}) \\ \quad (z<0), \end{cases}$$
$$K_{(1,2,3)z}\equiv(\omega_0/c)\left(\varepsilon_{(1,2,3)}-\varepsilon_1\sin^2\theta_0\right)^{1/2}$$
$$=\mathrm{i}(\omega_0/c)\left(\varepsilon_1\sin^2\theta_0-\varepsilon_{(1,2,3)}\right)^{1/2}, \quad (2)$$

where $n_1\,(\omega_0/c)\sin\theta_0=K_{1x}\equiv K_x$ is the x-component of the wave vector of the incoming field. If θ_0 is larger than the angle of total reflection θ_t (defined by the equation $n_3=n_1\sin\theta_t$, and $\theta_t=41.81^\circ$ in our case), then $K_{3z}=+\mathrm{i}|K_{3z}|$ is purely imaginary, and G_3 corresponds to an evanescent wave in region 3. The wave functions given by Equation (2) represent the electromagnetic field configuration induced by an incoming radiation whose electric field strength reads

$$\boldsymbol{E}_0=(\boldsymbol{e_x}\cos\theta_0+\boldsymbol{e_z}\sin\theta_0)|F_0|$$
$$\times\cos\left[\omega_0\left(t-n_1\frac{x\sin\theta_0-z\cos\theta_0}{c}\right)+\varphi_0\right], \quad (3)$$

where φ_0 is the phase of the complex amplitude F_0.

The wave functions $B_{\mathrm{sp}}(z)$ of the SPO eigenmodes look similar to $B_0(z)$ of Equation (2), but there are also crucial differences between them. On one hand, they do not contain the inhomogenity term, and, on the other hand, they are evanescent both in regions 1 and 3, i.e. they are bound to both of the interfaces, moreover, in general they spatially decay along the positive x-direction. The mode function of the SPO reads

$$B_{\mathrm{sp}}(z)\equiv\begin{cases} n_1f_1\exp(-k_{1z}z) & (z>d), \\ n_2(g_2\exp(k_{2z}z)+f_2\exp(-k_{2z}z)) & (0<z<d), \\ n_3g_3\exp(k_{3z}z) & (z<0), \end{cases}$$
$$k_{(1,2,3)z}=\left(k_{1x}^2-(\omega/c)^2\varepsilon_{(1,2,3)}\right)^{1/2}$$
$$\equiv(\omega/c)\left(\varepsilon_1\sin^2\theta'-\varepsilon_{(1,2,3)}\right)^{1/2} \quad (4)$$

Downloaded By: [Kroo, Norbert] At: 06:04 2 August 2010

Downloaded By: [Kroo, Norbert] At: 06:04 2 August 2010

with $k_{1x} \equiv k_{sp}$ and $\mathrm{Re}[k_{(1,3)z}] > 0$. In Equation (4) we have introduced the complex angle θ' by the definition $k_{sp} \equiv (\omega/c) n_1 \sin\theta'$ in order to emphasise the *formal* analogy between the formulas to that of Equation (2). From the set of four linear algebraic equations, obtained from the boundary conditions, the amplitudes F_1, G_2 and F_2 can be expressed in terms of G_3, where

$$G_3 = (4n_1 B/n_3)\exp[\mathrm{i}(K_{2z} - K_{1z})d] F_0/D_0,$$
$$D_0 \equiv (A+1)(B+1) - (A-1)(B-1)\exp(2\mathrm{i}K_{2z}d), \quad (5a)$$

$$F_1 = [(A+1)(B-1) - (A-1)(B+1)\exp(2\mathrm{i}K_{2z}d)] \cdot F_0 \exp(-2\mathrm{i}K_{1z}d)/D_0,$$
$$F_2 = (n_3/2n_2)(1-A)G_3, \quad (5b)$$

$$G_2 = (n_3/2n_2)(1+A)G_3,$$
$$A \equiv (n_2K_2/K_{2z})(K_{3z}/n_3K_3),$$
$$B \equiv (n_2K_2/K_{2z})(K_{1z}/n_1K_1). \quad (5c)$$

Similarly, f_1, g_2 and f_2 can be expressed in terms of g_3, but now, in the homogeneous case we have an indeterminate equation for g_3, $0 = D_{sp} \cdot g_3$,

$$D_{sp} \equiv (a+1)(b+1) - (a-1)(b-1)\exp(-2k_{2z}d), \quad (6a)$$

$$f_1 = [(1+a) + (1-a)\exp(-2k_{2z}d)] \cdot g_3 \exp(+k_{2z}d + k_{1z}d),$$
$$f_2 = (n_3/2n_2)(1-a)g_3, \quad (6b)$$

$$g_2 = (n_3/2n_2)(1+a)g_3,$$
$$a \equiv (n_2k_2/k_{2z})(k_{3z}/n_3k_3),$$
$$b \equiv (n_2k_2/k_{2z})(k_{1z}/n_1k_1). \quad (6c)$$

The determinants D_0 and D_{sp} defined in Equations (5a) and (6a), respectively, correspond to two distinct, mathematically and physically different situations. The scattering problem can have a physically acceptable solution only if $D_0 \neq 0$ (in the expression of G_3 in Equation (5a), the denominator must not be zero). On the other hand, the homogeneous problem (corresponding to the free eigenoscillations of the dielectric–metal–dielectric system) can have nontrivial solutions only if the determinant $D_{sp} = 0$ vanishes. As is well known, this latter condition defines the propagation constant $k_{sp}(\omega)$ of the SPO through a transcendental equation. If $|k_{2z}d| \gg 1$ (i.e. in the case of a relatively thick layer), according to Equation (6a), the condition $D_{sp} = 0$ becomes approximately the equation $a = -1$ (from which the well known implicit dispersion relation $k_{sp} = (\omega/c)[\varepsilon_2\varepsilon_3/(\varepsilon_2+\varepsilon_3)]^{1/2}$ can be derived). Quite similarly, if in Equation (5a) $|\exp(2\mathrm{i}K_{2z}d)| \ll 1$, then the determinant D_0 (and hence the denominator in the expression for G_3) gets close to zero if A approaches -1. If we take $\varepsilon_2 = -\varepsilon_R + \mathrm{i}\varepsilon_I$, with both ε_R and ε_I positive, and, moreover if we assume that $\varepsilon_I \ll \varepsilon_R$, then in the exponent we have approximately $-(4\pi d/\lambda_0)(\varepsilon_R+1)^{1/2}$. The factor in front of the square root is 0.711 in our case, where $d = 45$ nm, and $\lambda_0 = 795$ nm, i.e. in cases we are interested in, the exponential factor is much less than unity ($\exp[-(4\pi d/\lambda_0)(\varepsilon_R+1)^{1/2}] = 0.025$ if we take $\varepsilon_R = 25.81$ for a gold layer). By varying the parameters of the incoming field the amplitudes may undergo a resonant change (e.g. enhancement) in the ranges where the determinant D_0 gets close to zero. The value of this determinant is governed by the parameters A and B, whose dependence on the angle of incidence θ_0 is displayed in Figure 2 in the special case $\varepsilon_1 = (1.5)^2$, $\varepsilon_2(\omega_0) = -\varepsilon_R + \mathrm{i}\varepsilon_I = -25.82 + \mathrm{i}1.63$ and $\varepsilon_3 = 1$. The numerical value of ε_2 has been taken from Johnson and Christy [41].

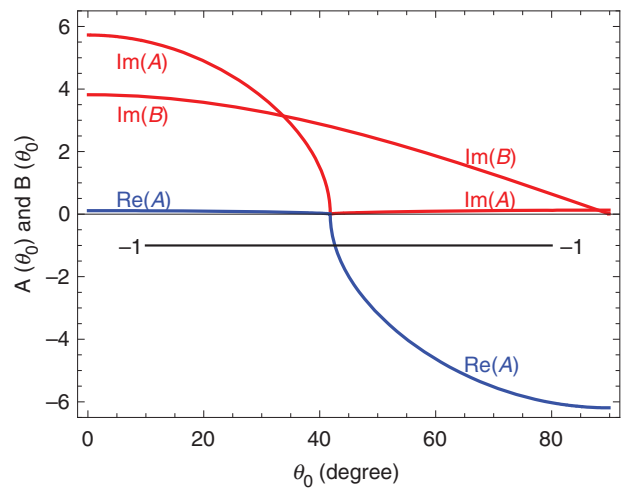

Figure 2. Shows the dependence on the angle of incidence θ_0 of the parameters A and B defined in the second row of Equation (5). Besides the θ_0-dependence, these parameters depend on the frequency of the incoming radiation through the permittivities. We have taken $\varepsilon_1 = 2.25$, $\varepsilon_2 = -25.81 + \mathrm{i}1.63$ and $\varepsilon_3 = 1$. We note that A and B do not depend on the thickness d of the metal layer. The dielectric in region 1 represents a glass substrate of index of refraction $n_1 = 1.5$, the metal layer in region 2 is assumed to be gold, and for region 3 we have taken vacuum. The numerical value of ε_2 has been taken from [41]. The exciting radiation field comes from a Ti:Sapphire laser of wavelength 795 nm whose photon energy is 1.5627 eV. The curves labelled by 'Im(A)', 'Re(A)' and 'Im(B)' represent the imaginary and the real part of A and the imaginary part of B, respectively. The horizontal thin line labelled by '−1' and represents the constant function $= -1$. At the angle of total reflection $\theta_t = 41.81°$ the parameter A changes from almost purely imaginary to almost purely negative real numbers, and at the critical angle $\theta_c = 42.84° = \theta_t + 1.03°$ its real part takes the value -1. The parameter B is almost purely imaginary throughout the whole angular range $0° < \theta_0 < 90°$, which is why we have not shown its real part. (The colour version of this figure is included in the online version of the journal.)

Downloaded By: [Kroo, Norbert] At: 06:04 2 August 2010

In Figure 3 we have plotted the relative modulus squared of the amplitudes of the induced field components as functions of the angle of incidence. At the critical angle $\theta_c = 42.84^\circ = \theta_t + 1.03^\circ$ the amplitude F_1 of the reflected wave drops practically to zero in a narrow angular range of half width of about 0.4°. In Figure 3(*a*) we see a clean example of the attenuated total reflection (ATR) in the Kretschmann geometry in the case of ideal plane interfaces. Figure 3(*d*) shows that around θ_c the transmitted intensity $\sim|G_3|^2$ undergoes a considerable resonant enhancement of magnitude ~150 relative to the incoming intensity $\sim|F_0|^2$. This phenomenon is usually interpreted as a consequence of the spatial compression at the metal–vacuum interface of the waves impinging from the other side onto the dielectric–metal interface and tunneling through the thin metal layer.

For small enough frequencies ($\omega_0 \ll \omega_p =$ plasma frequency) the dispersion relation of the SPO approximately coincides with that of a free plane wave of light propagating in vacuum. If $\omega \approx \omega_0$, then the resonance condition $D_0 \ll 1$ at $\theta_0 = \theta_c$ for the determinant defined in Equation (5) is essentially equivalent to the dispersion relation $D_{sp} = 0$ of the SPO (see Equation (6)), provided we make the replacement $k_{sp} \approx K_x = (\omega_0/c) \times n_1 \sin\theta_c \approx \omega_0/c$. In this case the parameters of the SPO approximately coincide with that of the forced oscillations, i.e. $a \approx A$ and $b \approx B$ (see the defining equations in Equations (5) and (6)). As is seen in Figure 3(*a*), the reflected field is practically zero, and the incoming laser field is converted to surface plasmon oscillations in the ATR process. In the case of 100% conversion efficiency [7], we assume $|g_3| \approx |G_3| = g|F_0|$, where we have introduced the enhancement factor g for the amplitudes. We have checked that at resonance the relative phase of G_3 and F_0 is zero, thus the SPO 'inherit' the phase of the incoming field, so we are allowed to take $g_3 \approx gF_0$.

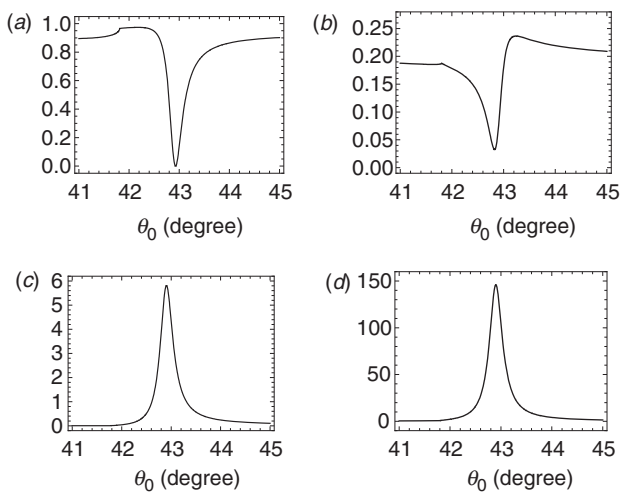

Figure 3. Shows the relative modulus squared of the amplitudes of the field configuration generated by an incoming plane wave as functions of the angle of incidence. Parts (*a*), (*b*), (*c*) and (*d*) show the intensities of the reflected, refracted, the secondary reflected and secondary refracted (transmitted) waves, respectively. The geometry of the scattering is illustrated in Figure 1. The thickness d of the metal layer has been taken to be $2 \times \delta = 45$ nm, the other parameters used in the calculations are the same as in Figure 1.

3. Dressed state of a metallic electron embedded in the enhanced field of SPOs

In the present section the SPO field is considered as a ('strong') classical external field, and its effect in the Schrödinger equation of the electron will be taken into account non-perturbatively. In general, one can say that in the frame of this kind of description the transition probability amplitudes of high-order plasmon absorption or emission processes can be obtained in a one-step perturbation calculation, where the perturbation represents the effect of the other ('weak') agents (e.g. as below in the next section, in the case of light emission by the SPO, the interaction with the quantised mode of the spontaneously emerging photon will be considered as a perturbation).

First of all we have to have the explicit form of the electric field strength of the SPO, which is to be inserted into the interaction term in the Schrödinger equation. From Equations (1), (4), (6b), (6c), and on the basis of the considerations at the end of the previous section, in the metal layer the wave numbers and the electric field strength of the SPO can be expressed as

$$k_{2x} = k_{sp} = \frac{\omega_0}{c}\left[1 + \frac{1}{2(\varepsilon_R - 1)} + \mathrm{i}\frac{\varepsilon_I}{2(\varepsilon_R - 1)^2}\right], \qquad k_{2z} = \frac{\omega_0(\varepsilon_R - 1)^{1/2}}{c}\left[1 + \mathrm{i}\frac{\varepsilon_I}{2(\varepsilon_R - 1)}\right], \tag{7a}$$

$$\begin{aligned} \boldsymbol{E}_{sp}(\boldsymbol{r}, t) = {} & g|F_0| \exp(-x/2L_{sp}) \exp(-z/2l_2) \\ & \times [(\varepsilon_R - 1)^{-1}\boldsymbol{e}_z \cos(\omega_0 t'' + \varphi_0) \\ & - (\varepsilon_R - 1)^{-1/2}\boldsymbol{e}_x \sin(\omega_0 t'' + \varphi_0)] \quad (0 < z < d), \end{aligned} \tag{7b}$$

$$L_{sp} \equiv |2\,\mathrm{Im}[k_{sp}]|^{-1} \approx \frac{(\varepsilon_R - 1)^2}{2\pi\varepsilon_I}\lambda_0, \tag{7c}$$

$$l_2 \equiv \frac{\lambda_0}{4\pi(\varepsilon_R - 1)^{1/2}} \quad t'' \equiv t - (n_1 \sin\theta_c)\frac{x}{c} + \frac{\varepsilon_I}{2(\varepsilon_R - 1)^{1/2}}\frac{z}{c}. \tag{7d}$$

Downloaded By: [Kroo, Norbert] At: 06:04 2 August 2010

The relative numerical accuracy of the above approximate expressions is of order of $\varepsilon_I/2(\varepsilon_R-1)^2$ (which is $\sim$0.001 in our case). In Equation (7c) we have introduced the 'propagation length' L_{sp} of the SPO (the $1/e$-length of the spatial energy distribution along the x-axis), which is $\sim 61.6\times\lambda_0 = 49\,\mu$m for $\varepsilon_R = 25.82$ and $\varepsilon_I = 1.63$. In the 'retarded time parameter' t'' introduced in Equation (7d) the factor $n_1 \sin\theta_c \approx 1 + 1/[2(\varepsilon_R - 1)]$ is practically unity (the resonance angle θ_c differs from the angle of total reflection θ_t only by about one degree). In region 3 (in vacuum), with the same accuracy as above, we have

$$k_{3x} = k_{sp} = \frac{\omega_0}{c}\left[1 + \frac{1}{2(\varepsilon_R - 1)} + \mathrm{i}\frac{\varepsilon_I}{2(\varepsilon_R-1)^2}\right],$$
$$k_{3z} = \frac{\omega_0}{c(\varepsilon_R-1)^{1/2}}\left[1 + \mathrm{i}\frac{\varepsilon_I}{2(\varepsilon_R-1)}\right], \tag{8a}$$

$$\boldsymbol{E}_{sp}(\boldsymbol{r},t) = g|F_0|\exp(-x/2L_{sp})\exp(z/2l_3) \times [\boldsymbol{e}_z\cos(\omega_0 t' + \varphi_0) - (\varepsilon_R - 1)^{-1/2}\boldsymbol{e}_x \sin(\omega_0 t' + \varphi_0)] \quad (z < 0), \tag{8b}$$

$$l_3 \equiv (\varepsilon_R - 1)^{1/2}\lambda_0/4\pi \quad t' \equiv t - (n_1\sin\theta_c)\frac{x}{c} - \frac{\varepsilon_I}{2(\varepsilon_R-1)^{3/2}}\frac{z}{c}. \tag{8c}$$

Thus, at the metal–vacuum interface the incoming field given by Equation (3) is transformed to SPO fields represented by Equations (7b) and (8b). Of course, these expressions are meant here only for positive values of x (in the frame of our description the SPO is generated at $x = 0$, where the electron, by scattering on a potential irregularity, converts energy from the enhanced evanescent wave to the surface plasmon oscillations, securing the extra momentum needed for the resonant coupling). We note that, according to our approximate analytic estimate, the enhancement factor g of the field amplitudes in Equations (7b) and (8b) behaves like $g \propto \exp[(2\pi d/\lambda_0)(\varepsilon_R + 1)^{1/2}]$ in the parameter range we are considering. We note that if we use the Drude free electron model [49], then we obtain $g \approx 30$ for the system under discussion.

It is seen in Equation (8b) that in vacuum the SPO has an elliptically polarised electric field whose longitudinal x-component is smaller by a factor of $(\varepsilon_R - 1)^{1/2} \approx 5$ than the z-component perpendicular to the metal surface. Inside the metal, on the other hand, the longitudinal component is larger by this same factor than the perpendicular one, so, this latter is smaller by a factor of $(\varepsilon_R - 1) \approx 25$ compared with its value in vacuum. The fields inside the metal exponentially drop to their $1/e$-value within the distance of $\lambda_0/31.3 \approx 25.4$ nm. In the 'retarded time parameters' t'' and t' defined in Equations (7c) and (8c), respectively, the factors of z/c are much smaller than unity, so henceforth in the phases of the field we shall use the common notation $t' \approx t - (n_1 \sin\theta_c)x/c$, i.e. $\omega_0 t' = \omega_0 t - K_x x$. In the following we set $\varphi_0 = 0$ for the initial phase, which means that possible carrier-envelope phase difference effects [13] are not discussed here (in the experiments we have used $\sim$120 fs 'long' pulses containing $\sim$46 cycles).

The Schrödinger equation of an electron interacting with the SPO field in the $\boldsymbol{r}\cdot\boldsymbol{E}$-gauge

$$\hat{H}_e\psi_e(\boldsymbol{r},t) = \mathrm{i}\hbar\partial_t\psi_e(\boldsymbol{r},t), \quad \hat{H}_e = \frac{\hat{\boldsymbol{p}}^2}{2m} + V(z) + e\boldsymbol{r}\cdot\boldsymbol{E}_{sp}, \tag{9}$$

where $\hat{\boldsymbol{p}} = -\mathrm{i}\hbar\nabla$ is the electron's momentum operator in coordinate representation, and the strong external field $\boldsymbol{E}_{sp}$ has been given in Equations (7b) and (8b). In the present paper we use the Sommerfeld step potential model for the metallic electrons, thus in the Hamiltonian given by Equation (9) we take $V(z) = V_0[\Theta(-z) - 1]$, i.e. $V(z) = 0$ for $z < 0$ and $V(z) = -V_0$ for $z > 0$. This means that we confine ourselves to the discussion of processes taking place at the metal–vacuum interface. The stationary solutions of the unperturbed Schrödinger equation of an electron are superpositions of plane waves,

$$\psi_e(\boldsymbol{r},t) = \langle \boldsymbol{r}|\boldsymbol{p}\rangle_t \equiv (1/L)\exp[(\mathrm{i}/\hbar)(p_x x + p_y y - Et)]\varphi_{E_z}(z), \tag{10a}$$

where $E = E_x + E_y + E_z$ and $E_{x,y} = p_{x,y}^2/2m \geq 0$. The function $\varphi_{E_z}(z)$ is a solution of the well known barrier problem of scattering on a step potential of depth $V_0 = E_F + A_w$ (see e.g. [42]), where E_F is the Fermi energy (=5.51 eV for gold) and A_w is the work function (=4.68 eV for gold), respectively. Depending on the energy associated with the z-motion, one has three kinds of solutions for the function $\varphi_{E_z}(z)$. We shall only need the form of $\varphi^{(0)}_{E_z}(z)$ for negative energies $(-V_0 \leq E_z < 0)$,

$$\varphi^{(0)}_{E_z}(z) = \left(\frac{m}{hp_0}\right)^{1/2}\begin{cases}\exp\left(-\frac{\mathrm{i}}{\hbar}p_0 z\right) + \frac{p_0 - \mathrm{i}q_0}{p_0 + \mathrm{i}q_0}\exp\left(+\frac{\mathrm{i}}{\hbar}p_0 z\right) \\ \quad \text{for } z > 0, \\ \frac{2p_0}{p_0 + \mathrm{i}q_0}\exp\left(+\frac{1}{\hbar}q_0 z\right) \\ \quad \text{for } z < 0,\end{cases} \tag{10b}$$

$$p_0 \equiv \left(2mV_0 - q_0^2\right)^{1/2}, \quad \frac{q_0^2}{2m} \equiv |E_z| = -E_z. \tag{10c}$$

The electron propagates freely both inside and outside the metal (except in the negative z-direction for energies $E_z < 0$, when its momentum is imaginary), the interaction is limited to the $z = 0$ plane, where the reflection and transmission may take place. In both

regions the fundamental solutions of Equation (9) can be taken as modulated plane waves of the form

$$\begin{aligned}\bar{\psi}_e(\boldsymbol{r},t) &= \langle \boldsymbol{r}-\boldsymbol{r}_{\rm cl}(t')|\boldsymbol{p}\rangle_{\rm t}\\ &= N\exp\{({\rm i}/\hbar)[\boldsymbol{p}\cdot(\boldsymbol{r}-\boldsymbol{r}_{\rm cl}(t'))-Et]\}\\ &\quad\times\exp[-{\rm i}h(t')],\end{aligned}\tag{11a}$$

$$\begin{aligned}\boldsymbol{r}_{\rm cl}(t') &\equiv \{x_{\rm cl}(t'),0,z_{\rm cl}(t')\}\\ x_{\rm cl}(t') &\equiv ag\mu_0\lambda\!\!\!^{-}_0\sin(\omega_0 t'),\\ z_{\rm cl}(t') &\equiv bg\mu_0\lambda\!\!\!^{-}_0\cos(\omega_0 t'),\end{aligned}\tag{11b}$$

$$\begin{aligned}a &= (\varepsilon_{\rm R}-1)^{-1/2},\\ b &= \begin{cases}(\varepsilon_{\rm R}-1)^{-1}, & 0<z<d,\\ 1, & z<0,\end{cases}\\ \mu_0 &\equiv (eF_0/mc\omega_0),\quad \mu_0^2 = 10^{-18}I_0\lambda_0^2,\end{aligned}\tag{11c}$$

where N is a normalisation factor. The real function $h(t')$ in the exponent on the right-hand side of Equation (11a) is a simple periodic function of the retarded time t', which drops out from the transition matrix elements to be calculated in the next section, so its explicit form is not of interest here. In region 3 ($z<0$) the z-component of the momentum of an evanescent electron is defined as

$$\begin{aligned}p_z &= -\left[2m(E_z-U_{\rm sp})\right]^{1/2},\\ U_{\rm sp} &\equiv g^2\mu_0^2(2mc^2)/8 = 5.14\times10^{-14}g^2I_0\lambda_0^2\quad (z<0),\end{aligned}\tag{12}$$

where the 'ponderomotive energy shift' $U_{\rm sp}$ of the electron comes as an average effect stemming from the SPO. This shift can play an important role in field enhanced multiphoton photoelectric emission from metal films [19,20]. $U_{\rm sp}$ is measured in eV if on the right-hand side of Equation (12) I_0 and λ_0 are measured in W cm^{-2} and μm, respectively. In Equation (11b) we have introduced the components of the classical trajectory $\boldsymbol{r}_{\rm cl}(t)$, along which the electron oscillates in the SPO field according to the Newton equation $m\ddot{\boldsymbol{r}}_{\rm cl} = -e\boldsymbol{E}_{\rm sp}$. The dimensionless 'intensity parameter' μ_0 introduced in Equation (11b) plays a crucial role in nonlinear processes. Its numerical value can be calculated from the last equation in Equation (11c), where the intensity I_0 and the central wavelength λ_0 of the incoming laser field are measured in W cm^{-2} and μm, respectively. It is important to note that in obtaining Equation (11a) the x-dependence in t' has been taken into account only parametrically, like in the dipole approximation (where we use mere time-dependence). Similarly, we have considered the smooth profile functions of the amplitudes, $\exp(-x/2L_{\rm sp})$ and $\exp(\mp z/2l_{2,3})$ merely as functions of the parameters x and z. This is justified if the amplitudes of the classical oscillations $x_{\rm cl}(t)$ and $z_{\rm cl}(t)$ are much smaller than the wavelength λ_0, which can be satisfied if $g\mu_0<1$. Concerning the method of parametric substitution (see [43–45]), where it has also been shown that the de Broglie wavelength of the free electron has to be considerably smaller than the wavelength of the radiation, for a reliable approximation. One can easily calculate that e.g. $\lambda_{\rm dB}/\lambda_0 = \hbar\omega_0/pc \sim 10^{-4}$ even for thermal electrons. We note that the dressed states shown in Equation (11a) are generalisations of the so-called Volkov states, which have been extensively used in the theory of strong-field laser–matter interaction phenomena from the very beginning [46]. An analogous but, on the other hand, a special form of these dressed states was first used by Bunkin and Fedorov [47] in their treatment of laser-induced cold emission (optical tunneling of electrons) from metal surfaces.

4. Photon emission during multiple-plasmon scattering by a metallic electron

In order to describe spontaneous light emission by the dressed electron, we have to solve the Schrödinger equation of the joint system of an electron interacting with the SPO field and the quantised EM field of the photons,

$${\rm i}\hbar\partial_{\rm t}|\Psi(t)\rangle = \hat{H}|\Psi(t)\rangle,\quad \hat{H} = \frac{\hat{\boldsymbol{p}}^2}{2m}+V(z)+e\boldsymbol{r}\cdot\boldsymbol{E}_{\rm sp}+e\boldsymbol{r}\cdot\hat{\boldsymbol{E}}_Q,\tag{13}$$

where $\hat{\boldsymbol{p}} = -{\rm i}\hbar\nabla$ is the electron's momentum operator, and the strong external field representing the surface plasmon oscillations, $\boldsymbol{E}_{\rm sp}$ has been given in Equations (7b) and (8b). For the electric field strength $\hat{\boldsymbol{E}}_Q$ of the spontaneously emitted radiation in vacuum we will take the following approximate form after Elson and Ritchie [34],

$$\begin{aligned}\hat{\boldsymbol{E}}_Q(\boldsymbol{r},t) &= \sum_{\boldsymbol{k}}\int {\rm d}k_z(4\hbar\omega/L^2)^{1/2}\\ &\quad\times\left[\hat{\boldsymbol{k}}(ck_z/\omega)\cos(k_zz+\eta)+{\rm i}\boldsymbol{e}_z(ck/\omega)\sin(k_zz+\eta)\right]\\ &\quad\times\left(\hat{a}^+_{\boldsymbol{k},k_z}\exp({\rm i}\omega t)-\hat{a}_{-\boldsymbol{k},k_z}\exp(-{\rm i}\omega t)\right)\exp(-{\rm i}\boldsymbol{k}\cdot\boldsymbol{r})\\ &\quad (z<0),\end{aligned}\tag{14a}$$

$$\begin{aligned}\boldsymbol{k} &\equiv (k_x,k_y,0)\equiv(k\sin\theta)\hat{\boldsymbol{k}} = (k\sin\theta)(\cos\varphi,\sin\varphi,0),\\ k_z &= (\omega/c)\cos\theta,\end{aligned}\tag{14b}$$

$$\begin{aligned}\omega &\equiv c\left(k^2+k_z^2\right)^{1/2},\\ \sin\eta &= \frac{k_z\varepsilon_{\rm R}}{\left[(\varepsilon_{\rm R}+1)(k^2+k_z^2\varepsilon_{\rm R})\right]^{1/2}},\\ [\hat{a}_{\boldsymbol{k},k_z},\hat{a}^+_{\boldsymbol{k}',k'_z}] &= \delta_{\boldsymbol{k},\boldsymbol{k}'}\delta(k_z-k'_z).\end{aligned}\tag{14c}$$

(We show the expression only for the p-polarised components, because – as will be proved below – the

Downloaded By: [Kroo, Norbert] At: 06:04 2 August 2010

Downloaded By: [Kroo, Norbert] At: 06:04 2 August 2010

emission of s-polarised photons are forbidden.) The summation and integration with respect to the wave numbers $\{\boldsymbol{k}, k_z\}$ of the emerging photons in Equation (14a) is limited to k-space regions where $\omega < \omega_p$, because the metal layer is transparent for larger frequencies, and the mode functions have a different form to that given here. The form of the quantised field in Equation (14a), given by Elson and Ritchie [34], corresponds to the approximation in which we consider a *semi-infinite lossless* metal ($\varepsilon_I = 0$) occupying the half-space $0 < z$. We have checked by a couple of numerical calculations that in the case of a *finite lossy* metal layer illustrated in Figure 1, the reflection coefficients of the quantised modes are not considerably less than unity. In particular, if the polar angle θ (with respect to the *negative* z-axis) is close to 90°, then the reflection coefficients are close to 100%, thus this approximation is justified (this is also supported *a posteriori* by the results obtained for the angular distributions of the spontaneously emitted photons, which peaks around ~70°). We also note that for higher order harmonics ($n\omega > \omega_p$) the dielectric–metal system is practically transparent, and then, to a good approximation, we can work with the usual free-space expression of the electric field strength of the quantised radiation [35],

$$\hat{\boldsymbol{E}}(\boldsymbol{r}, t) = \mathrm{i} \sum_{\boldsymbol{k}, s} \boldsymbol{e}_s(\boldsymbol{k})(2\pi\hbar\omega/L^3)^{1/2}\Big[\hat{a}_{\boldsymbol{k}, s} \exp[\mathrm{i}(\boldsymbol{k}\cdot\boldsymbol{r} - \omega t)] - \hat{a}^{+}_{\boldsymbol{k}, s} \exp[-\mathrm{i}(\boldsymbol{k}\cdot\boldsymbol{r} - \omega t)]\Big], \tag{15}$$

where the subscript 's' refers to the two independent linear polarisations belonging to the propagation vector $\boldsymbol{k} = (k_x, k_y, k_z)$. Concerning the mode density, one essential difference between Equations (14a), (14b), (14c) and (15) can be immediately seen, namely the presence of the extra factors $ck_z/\omega = k_z/(k^2 + k_z^2)^{1/2}$ and $ck/\omega = k/(k^2 + k_z^2)^{1/2}$ on the right-hand side of Equation (14b). These factors are partly responsible for the modification of the kinematics (in other words, for the modification of the angular distribution) of the spontaneous emission, due to the presence of the metal boundary. The transition matrix elements of the spontaneous emission can be calculated in a very similar manner as has been done in the earlier works of one of us [31,32]. For the initial and final states of the electron we take dressed states of the type given in Equation (11a)

$$\begin{aligned} T_{\mathrm{fi}} &= -(\mathrm{i}/\hbar)\int_{-\infty}^{\infty} \mathrm{d}t \langle \bar{\psi}_{\mathrm{ef}} | [\boldsymbol{e}\cdot\nabla V(z)] | \bar{\psi}_{\mathrm{ei}} \rangle \exp[(\mathrm{i}/\hbar)(E' - E)t] \\ &\quad \times (e/m\omega^2)(4\hbar\omega/L^2)^{1/2}(ck/\omega) \\ &\quad \times \sin(kz + \eta)\exp[\mathrm{i}(\omega t)] \\ &= -2\pi\mathrm{i}\sum_n t_{\mathrm{fi}}^{(n)}\delta(E - E' + n\hbar\omega_0 - \hbar\omega), \end{aligned} \tag{16}$$

where the Dirac delta expresses the conservation of energy $E' + \hbar\omega = E + n\hbar\omega_0$. This means, that n plasmons are absorbed by the electron and the energy is converted to the sum of the final electron energy and the energy of the spontaneously emitted photon. If the change in the electron's energy is small, then the spectrum of the emitted radiation is peaked at the harmonic frequencies $\omega = n\omega_0$. This is the case in *specular electron reflection* at the metal–vacuum interface. If we do not assume this specular reflection, then, in the frame of the present description, we cannot account for the narrow spectra measured in the experiments. The sum with respect to n in Equation (16) has been derived from the Fourier expansion of the periodic modulation factors in the dressed states by taking Equations (11a) and (11b) into account, and using the Jacobi–Anger formula $\exp(\mathrm{i}z\sin\varphi) = \sum_{n=-\infty}^{\infty} J_n(z)\exp(\mathrm{i}n\cdot\varphi)$, where $J_n(z)$ denotes the ordinary Bessel function of the first kind of order n [48]. From Equation (16) we immediately see that *the emission of s-polarized photons are forbidden* (the gradient of $V(z)$ is necessarily pointing to the z-direction, so a vector $\boldsymbol{e}$ in the plane of the interface is of course orthogonal to that). On the basis of Equation (16) the production rates of the nth harmonic photons can be brought to the form

$$\begin{aligned} \frac{\mathrm{d}P_n}{\mathrm{d}\Omega} &= \nu_0\alpha f^2(\theta)G^2(\upsilon) \\ &\quad \times \Bigg| \sum_k nF(u_{n+k})J_{n+k}[ag\mu_0(c/\hbar\omega_0)(p_x - p'_x)] \\ &\quad \times I_k[g\mu_0(c/\hbar\omega_0)(|p_z| + |p'_z|)]\Bigg|^2, \end{aligned} \tag{17}$$

$$f(\theta) \equiv \frac{2\varepsilon_{\mathrm{R}}(\sin 2\theta)}{\left[(\varepsilon_{\mathrm{R}} + 1)(\sin^2\theta + \varepsilon_{\mathrm{R}}\cos^2\theta)\right]^{1/2}}, \tag{17a}$$

$$\begin{aligned} F(u_{n+k}) &\equiv \frac{1}{1 + \mathrm{i}u_{n+k}}, \\ u_{n+k} &\equiv 2[p_x - p'_x + (n+k)\hbar K_x - \hbar k_x]L_{\mathrm{sp}}/(n+k)\hbar, \end{aligned} \tag{17b}$$

$$G(\upsilon) \equiv \frac{\sin\upsilon}{\upsilon}, \quad \upsilon \equiv (p_y - p'_y - \hbar k_y)L/\hbar, \tag{17c}$$

where $\alpha = e^2/\hbar c \cong 1/137$ is the fine structure constant, and $\nu_0 = \omega_0/2\pi$. In obtaining Equation (17) we have used the relation $J_n(\mathrm{i}z) = \mathrm{i}^n I_n(z)$, which connects the ordinary Bessel functions $J_n(z)$ and the modified Bessel functions $I_n(z)$ of the first kind of integer order. In order to complete the calculation, the above formula for the production rate still should be integrated with respect to the possible initial and final electron

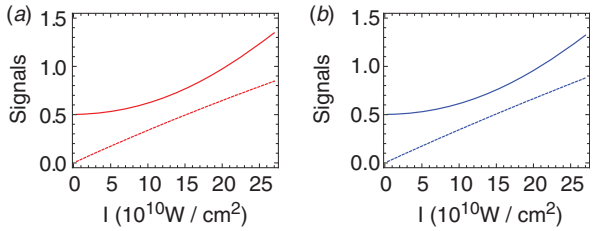

Figure 4. Shows the intensity dependence of the fundamental (*a*) and the second harmonic (*b*) dimensionless production rates $(\mathrm{d}P_n/\mathrm{d}\Omega)/(3\times10^{-5}\alpha\nu)$ according to the formula given by Equation (17) at $\theta=\theta_{\max}$. The dashed and the full lines refer to results with no field enhancement and with enhancement of magnitude $g^2=150$. Because the enhanced signals are much larger than the signals with no enhancement, we have divided their value by 1500 for the fundamental and by 1450 for the second harmonics, respectively. The dashed lines show that in the intensity range we have considered the linear dependence is reproduced, which comes out when one treats the SPO field perturbatively, though the second harmonic also shows almost linear behaviour. This is because the interference terms in Equation (17) are playing an important role. The strong deviation from the perturbative results are clearly seen. (The colour version of this figure is included in the online version of the journal.)

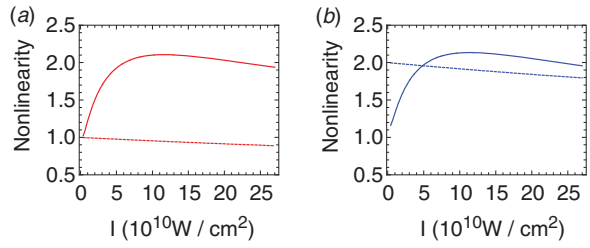

Figure 5. In this we show the dependence of the 'degree of nonlinearity', $\partial\log S/\partial\log I$, where S stands for the signal intensity. The labelling of the curves are the same as in Figure 4. In the case of no enhancement, the slope of the signals gives a perturbative dependence. The dashed lines show that (*a*) $\partial\log S_1/\partial\log I\cong1$ and (*b*) $\partial\log S_2/\partial\log I\cong2$ in the whole intensity range. This corresponds to the well known perturbative results, $S_1\sim I$ for the fundamental radiation, and $S_2\sim I^2$ for the second harmonic. The degree of nonlinearity of the enhanced signals strongly deviate from the perturbative results in a complicated way. (The colour version of this figure is included in the online version of the journal.)

momenta $\boldsymbol{p}$ and $\boldsymbol{p}'$, respectively, by taking into account the conservation of energy $E'+\hbar\omega=E+n\hbar\omega_0$ and the corresponding Fermi distribution. This has been approximately done in a similar case in [31], with the conclusion that this procedure leads to a spreading in energy of order of $\Delta E\approx4\times kT\approx0.1\,\mathrm{eV}$ (at room temperature, $T=293\,\mathrm{K}$, $kT\approx0.025\,\mathrm{eV}$). The relative energy spread $\Delta E/E_{\mathrm{F}}\approx0.018$ would correspond to the spectral width $\Delta\lambda\approx0.018\times\lambda_0=14.3\,\mathrm{nm}$, which is quite close to the experimental value [38]. In Equation (17) $G^2(\upsilon)$ vanishes for $L\to\infty$, unless k_y is zero. Thus, the

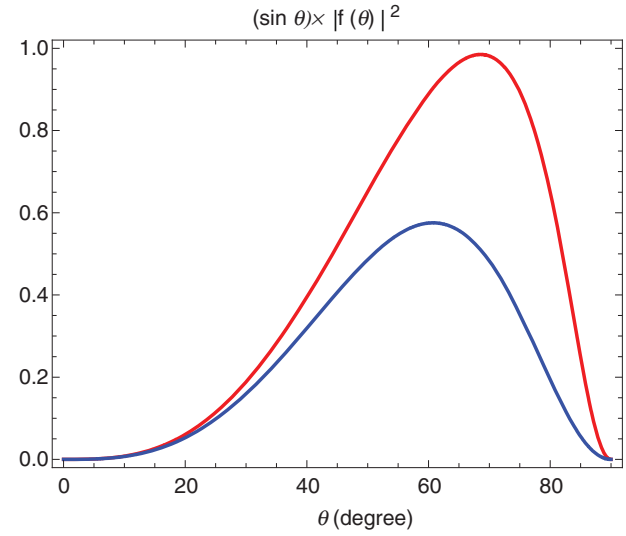

Figure 6. Shows the angular dependence of the fundamental (red curve) and the second harmonic (blue curve) normalised photon production rates in the low-intensity case, when $I_0=10^{10}\,\mathrm{W\,cm^{-2}}$ has been assumed, and the enhancement factor has been taken to be $g=150^{1/2}$. In the figure the function $1.6\times(\sin\theta)|f(\theta)|^2$ has been plotted on the basis of the defining equation, Equation (17a). For the quantitative difference between the curves the use of the different dielectric constants is responsible. For $\omega=\omega_0$ the value $\varepsilon_{\mathrm{R}}=25.82$, and for $\omega=2\omega_0$ the value $\varepsilon_{\mathrm{R}}=5.71$ has been taken. (The colour version of this figure is included in the online version of the journal.)

wave vector of the emitted photon lies in the x–z plane (the scattering plane). In Equation (17) the angle between the negative z-axis and the k-vector of the emitted photon is denoted by θ, thus its wave vector has the form $\boldsymbol{k}=(\omega/c)(\sin\theta,\ 0,\ \cos\theta)$. In the rest of the present section we give some illustrations of the numerical results on the basis of the formula for the differential production rates given by Equation (17).

The dashed lines in Figure 4 show that in the intensity range we have considered the linear dependence to be reproduced, which comes out when one treats the SPO field perturbatively. The strong deviation from the perturbative results are clearly seen. It is remarkable that the enhanced signals do not saturate, at least in this intensity range, rather, their slope remains positive for large intensities. This behaviour is in agreement with our measurements [38].

As is shown in Figure 5, without enhancement, the well known perturbative results are reproduced, i.e. $S_1\sim I$ for the fundamental, and $S_2\sim I^2$ for the second harmonic radiation. On the other hand, the degree of nonlinearity of the signals stemming from the enhanced field, strongly deviates from the perturbative results in a complicated way.

It can be shown that for low intensities of the incoming radiation (when e.g. $\mu_0=10^{-4}$ for a

Downloaded By: [Kroo, Norbert] At: 06:04 2 August 2010

Ti:Sapphire laser of intensity $I_0 = 10^{10}\,\mathrm{W\,cm^{-2}}$), even by taking into account the field enhancement, the angular distribution of the emitted light is essentially governed by the function $f(\theta)$ defined in Equation (17a). This function does not depend on the intensity, but it is sensitive to the frequency through the frequency-dependent permittivity $\varepsilon_2(\omega)$. In Figure 6 we have plotted the angular distributions of the fundamental ($\varepsilon_R = 25.82$) and of the second harmonic ($\varepsilon_R = 5.71$) signals, by using exclusively the function $f(\theta)$.

According to this Figure 6, the distribution of the fundamental radiation is peaked around $\theta^{(1)}_{\max} = 70^\circ$, and the second harmonic has a maximum at about $\theta^{(2)}_{\max} = 60^\circ$, and this latter is broader than the former one. For the detailed discussion of the angular distribution for larger incoming intensities than $\sim 10^{10}\,\mathrm{W\,cm^{-2}}$ we have to thoroughly investigate the numerical behaviour of the sum of the products of the Bessel functions in the formula of the production rates given by Equation (17). This will be one of the subjects of our future work concerning non-linear surface plasmonics.

5. Summary

In the present paper we have given a theoretical analysis of the enhanced surface-plasmon-assisted spontaneous radiation of a metallic electron. First, in Section 2 we have discussed the kinematics of the generation of the occasionally very high-intensity evanescent electromagnetic fields and surface plasmon oscillations at the metal–vacuum interface of a dielectric–metal–vacuum system. We have determined the spatial distribution and the amplitude of this field, and have given a couple of numerical examples which are relevant in our recent experiments. In Section 3, after having determined the interaction term to be put into the Schrödinger equation, the dressed quantum states of the electrons embedded into the high-intensity SPO field have been derived. In Section 4, on the basis of these dressed states, we have determined in a one-step perturbation calculation the transition matrix elements of the multiple-plasmon-assisted spontaneous emission of photons in the SPO environment. Here we have given a general formula for the absolute production rates of the harmonic components for arbitrary high order. As a first result, it follows from our theory that the emitted radiation must exclusively be p-polarised, in agreement with the experiments. We have made an estimate on the relative bandwidth of the radiation, and illustrated the unusual characteristics of the emitted radiation with the help of some typical numerical examples, as applications of our analytic results. It has turned out that, due to the large enhancement of the exciting laser fields in the vicinity of the interfaces, a considerable distortion of the intensity distribution of the signal appears, like in our recent experiments. Finally, we have given a special example, relevant only in the low-intensity case, for the angular distribution of the emitted fundamental and second harmonic radiation. In general, we have found a good qualitative agreement between the predictions of the present theory and our recent experimental findings on enhanced and nonlinear light emission at metal surfaces. According to the apparent harmony between theory and experiment, we conjecture that the light signals measured in our recent experiment are stemming from multiple SPO conversion during the scattering on the free electrons which are reflected specularly at the metal surface.

We think that the theoretical method presented here may also find applications in analysing other plasmon-induced nonlinear processes, like for instance high-order electron emission from thin metal films.

Acknowledgements

This work has been supported by the Hungarian National Scientific Research Foundation OTKA, Grant No. K73728. The authors thank the unknown referees for the constructive critics and for many valuable suggestions made by them, most of which have been taken into account in the final version of the present paper.

Note

1. Stratton [1] writes at the beginning of Section 9.28 of his book that 'The classical investigation of the effect of a finitely conducting plane upon the radiation of an oscillating dipole was published by Arnold Sommerfeld in 1909. Since that time an enormous amount of work has appeared on the subject and it may be fairly said no aspect of the problem of radio wave propagation has received more careful attention.' On pp. 584–585 a brief summary of the early history of electromagnetic surface waves is given, and in Section 9.28 a detailed discussion of the problem is presented. Section 11 of Sommerfeld's fundamental paper [2] is devoted to the discussion of the analogies between the propagation of *radio waves* and *optical waves* in the vicinity of a plane interface separating a dielectrics and a conducting medium (metal). This was the first hint that surface waves may play an important role in the visible part of the electromagnetic spectrum.

References

[1] Stratton, J.A. *Electromagnetic Theory*; Wiley: New Jersey, 2007.
[2] Sommerfeld, A. *Ann. Phys.* **1909,** *28,* 665–736.
[3] Burstein, E.; de Martini, F., Eds. *Polaritons*; Pergamon: London, 1974.

Downloaded By: [Kroo, Norbert] At: 06:04 2 August 2010

[4] Maradudin, A.A.; Agranovich, V.M.; Mills, D.L., Eds. *Surface Polaritons*; North-Holland: Amsterdam, 1982.
[5] Raether, H. *Excitation of Plasmons and Interband Transitions by Electrons*; Springer: Berlin, 1980; Raether, H. *Surface Plasmons*, Springer: Berlin, 1988.
[6] Zayats, A.V.; Smolyaninov, I.I. *J. Opt. A: Pure Appl. Opt.* **2003,** *5,* S16–S50.
[7] Zayats, A.V.; Smolyaninov, I.I.; Maradudin, A.A. *Phys. Rep.* **2005,** *408,* 131–314.
[8] Stockman, M.I.; Faleev, S.V.; Bergman, D.J. *Phys. Rev. Lett.* **2001,** *87,* 167401.
[9] Altewischer, E.; van Exter, M.P.; Woerdman, J.P. *Nature* **2002,** *418,* 304–306.
[10] Barnes, W.L.; Dereux, A.; Ebbesen, T.W. *Nature* **2003,** *424,* 824–830.
[11] Irvine, S.E.; Elezzabi, A.Y. *Appl. Phys. Lett.* **2005,** *86,* 264102.
[12] Fasel, S.; Halder, M.; Gisin, N.; Zbinden, H. *New J. Phys.* **2006,** *8,* 13.
[13] Irvine, S.E.; Dombi, P.; Farkas, Gy.; Elezzabi, A.Y. *Phys. Rev. Lett.* **2006,** *97,* 146801.
[14] Chau, K.J.; Johnson, M.; Elezzabi, A.Y. *Phys. Rev. Lett.* **2007,** *98,* 133901.
[15] Stockman, M.I.; Kling, M.F.; Kleineberg, U.; Krausz, F. *Nature Photon.* **2007,** *1,* 539–544.
[16] Min, B.; Ostby, E.; Sorger, V.; Ulin-Avila, E.; Yang, L.; Zhang, X.; Vahala, K. *Nature* **2009,** *457,* 455–458.
[17] Brongersma, M.L.; Kirk, P.G., Eds. *Surface Plasmon Nanophotonics*; Springer: Dordrecht, 2007.
[18] Fano, U. *Ann. Phys.* **1938,** *32,* 393–443.
[19] Tsang, T.; Srinivasan-Rao, T.; Fischer, J. *Phys. Rev. B* **1991,** *43,* 8870–8878.
[20] Aeschlimann, M.; Schmuttenmaer, C.A.; Elsayed-Ali, H.E.; Miller, R.J.D.; Cao, J.; Mantell, D.A. *J. Chem. Phys.* **1995,** *102,* 8606–8613.
[21] Roth, M.R.; Panoiu, C.N.; Adams, M.M.; Osgood Jr, M.R. *Opt. Express* **2006,** *14,* 2921–2931.
[22] Kim, S.; Jin, J.; Kim, Y.-J.; Park, I.-Y.; Kim, Y.; Kim, S.-W. *Nature* **2008,** *453,* 757–760.
[23] Wu, J.; Qi, H.; Zeng, H. *Phys. Rev. A* **2008,** *77,* 053412.
[24] Lu, P.; Wu, J.; Qi, H.; Zeng, H. *Appl. Phys. Lett.* **2008,** *93,* 201108.
[25] Wu, J.; Qi, H.; Zeng, H. *Appl. Phys. Lett.* **2008,** *93,* 051103.
[26] L'Huillier, A.; Schaefer, K.J.; Kulander, K. *J. Phys. B. At. Mol. Opt. Phys.* **1991,** *24,* 3315.
[27] Lewenstein, M.; Balcou, P.; Ivanov, M.Yu.; L'Huillier, A.; Corkum, P.B. *Phys. Rev. A* **1994,** *49,* 2117–2132.
[28] Krausz, F.; Ivanov, M. *Rev. Mod. Phys.* **2009,** *81,* 163–234.
[29] Barnes, W.L. *J. Mod. Opt.* **1998,** *45,* 661–699.
[30] von der Linde, D.; Engers, T.; Jenke, G.; Agostini, P.; Grillon, G.; Nibbering, E.; Mysyrowicz, A.; Antonetti, A. *Phys. Rev. A* **1995,** *52,* R25–R27.
[31] Varró, S.; Ehlotzky, F. *Phys. Rev. A* **1994,** *49,* 3106–3109.
[32] Varró, S.; Ehlotzky, F. *Phys. Rev. A* **1996,** *54,* 3245–3249.
[33] Kretschmann, E.; Raether, H. *Z. Naturforsch.* **1968,** *23A,* 2135–2136.
[34] Elson, J.M.; Ritchie, R.H. *Phys. Rev. B* **1971,** *4,* 4129–4138.
[35] Bergou, J.; Varró, S. *J. Phys. A: Math. Gen.* **1981,** *14,* 2281–2303.
[36] Kroó, N.; Varró, S.; Farkas, Gy.; Dombi, P.; Oszetzky, D.; Nagy, A.; Czitrovszky, A. *J. Mod. Opt.* **2007,** *54,* 2679–2688.
[37] Kroó, N.; Varró, S.; Farkas, Gy.; Dombi, P.; Oszetzky, D.; Nagy, A.; Czitrovszky, A. *J. Mod. Opt.* **2008,** *55,* 3203–3210.
[38] Kroó, N.; Farkas, Gy.; Dombi, P.; Varró, S. *Opt. Express* **2008,** *16,* 21656–21661.
[39] Economou, E.N. *Phys. Rev.* **1969,** *182,* 539–554.
[40] Burke, J.J.; Stegeman, G.I.; Tamir, T. *Phys. Rev. B* **1986,** *33,* 5186–5201.
[41] Johnson, P.B.; Christy, R.W. *Phys. Rev. B* **1972,** *6,* 4370–4379.
[42] Bohm, D. *Quantum Theory*; Prentice-Hall: Englewood Cliffs, 1957; Chapter 11.
[43] Bergou, J.; Varró, S. *J. Phys. A: Math. Gen.* **1981,** *13,* 3553–3559.
[44] Drühl, K.; McIver, J.K. *J. Math. Phys.* **1983,** *24,* 705.
[45] Reiss, H. *Phys. Rev. A* **2000,** *63,* 013409.
[46] Kylstra, N.; Joachain, C.J.; Dörr, M. In *Atoms, Solids and Plasmas in Super-intense Laser Fields*; Batani, D., Joachain, C.J., Martellucci, S., Chester, A.N., Eds.; Kluwer: New York, 2001; pp 15–36.
[47] Bunkin, F.V.; Fedorov, M.V. *Sov. Phys. JETP* **1965,** *21,* 896.
[48] Erdélyi, A., Ed. *Higher Transcendental Functions*; McGraw-Hill: New York, 1953; Vol. II, Formula 7.2.4(26).
[49] Born, M.; Wolf, E. *Principles of Optics*; Pergamon: London, 1959; Section 13.3.

Downloaded By: [Kroo, Norbert] At: 06:04 2 August 2010